



Steady-state kinetic analysis of halogenase-supporting flavin reductases BorF and AbeF reveals different kinetic mechanisms

Aravinda J. De Silva¹, Rippa Sehgal¹, Jennifer Kim, John J. Bellizzi III*

Department of Chemistry and Biochemistry, College of Natural Sciences and Mathematics, The University of Toledo Toledo, OH, 43606, USA



ARTICLE INFO

Keywords:
Oxidoreductase
Steady-state kinetics
FAD
NADH

ABSTRACT

The short-chain flavin reductases BorF and AbeF reduce FAD to FADH₂, which is then used by flavin-dependent halogenases (BorH and AbeH respectively) to regioselectively chlorinate tryptophan in the biosynthesis of indolotryptoline natural products. Recombinant AbeF and BorF were overexpressed and purified as homodimers from *E. coli*, and copurified with substoichiometric amounts of FAD, which could be easily removed. AbeF and BorF can reduce FAD, FMN, and riboflavin *in vitro* and are selective for NADH over NADPH. Initial velocity studies in the presence and absence of inhibitors showed that BorF proceeds by a sequential ordered kinetic mechanism in which FAD binds first, while AbeF follows a random-ordered sequence of substrate binding. Fluorescence quenching experiments verified that NADH does not bind BorF in the absence of FAD, and that both AbeF and BorF bind FAD with higher affinity than FADH₂. pH-rate profiles of BorF and AbeF were bell-shaped with maximum k_{cat} at pH 7.5, and site-directed mutagenesis of BorF implicated His160 and Arg38 as contributing to the catalytic activity and the pH dependence.

1. Introduction

Reduced flavins act as electron donors in a variety of reactions involving O₂, including hydroxylation, epoxidation, halogenation, and bioluminescence [1–4]. Oxidoreductases belonging to the two-component flavin-dependent monooxygenase and halogenase families use reduced flavin but are unable to reduce it themselves [5,6]. Instead, unlike true flavoenzymes, they release oxidized flavin as a product, which is taken up by a separate flavin reductase (FR) enzyme that reduces the flavin to complete the catalytic cycle.

FRs catalyze the reduction of flavins, including riboflavin, flavin mononucleotide (FMN) and flavin adenine dinucleotide (FAD), using NADH or NADPH as a source of electrons. They may be categorized on the basis of nicotinamide cofactor selectivity (NADH specific, NADPH specific, or both) [7]. Alternatively, they can be classified based on whether or not the FR uses a flavin cofactor that acts as an intermediate electron carrier between the nicotinamide electron donor and the oxidized flavin substrate (Type I FRs) or instead catalyzes direct reduction of oxidized flavin substrate by the nicotinamide in a ternary complex (Type II FRs) [7,8]. This distinction gives rise to different kinetic mechanisms for different FRs, with the Type I enzymes using a

ping-pong bi mechanism in which NAD(P)H reduces the flavin cofactor, followed by reduced flavin cofactor reducing the oxidized flavin substrate, and the Type II FRs using a sequential mechanism involving a ternary complex with direct hydride transfer from NAD(P)H to the oxidized flavin substrate.

The ability of flavin-dependent halogenases to carry out regioselective aryl halide synthesis under green chemistry conditions has led to a great deal of interest in their use as *in vitro* biocatalysts, but they suffer from relatively low turnover numbers and limited stability and catalytic lifetime [1,9–15]. Protein engineering and directed evolution approaches to improve the *in vitro* stability and performance of halogenase systems have mostly focused on the halogenase subunits rather than the flavin reductases [11,16–20].

The FRs that provide reduced flavin to two-component monooxygenase and halogenase systems belong to a family of short-chain oxidoreductases (InterPro IPR002563; Pfam PF01613; SMART SM00903) [21]. Most of these FRs from two-component systems are specific for NADH over NADPH and many can reduce FAD, FMN, or riboflavin, placing them in EC category 1.5.1.36. Most two-component monooxygenase systems appear to transfer flavin between subunits by free diffusion [22]. Since the halogenases can take up FADH₂ from

* Corresponding author.

E-mail address: john.bellizzi@utoledo.edu (J.J. Bellizzi).

¹ Equal contribution.

solution, any enzymatic or chemical source of FADH₂ can be used, and many *in vitro* halogenation reactions have used flavin reductases other than the specific reductase partner of the halogenase (for example, *E. coli* Fre) [23–27]. However, freely diffusing FADH₂ can react with O₂ and other oxidants in solution, leading to side reactions and decreasing the overall catalytic efficiency.

Several studies suggest that the catalytic efficiency of two-component halogenase systems can be improved by optimization of flavin reduction and transfer. As demonstrated for the tryptophan-6-halogenase Thal, formation of a halogenase/reduced flavin complex in the absence of substrate can lead to HOCl leakage as well as the formation of a catalytically inactive complex, suggesting that reaction conditions generating excess FADH₂ will be counterproductive to efficient halogenation [28]. It has also been shown that physically linking FR and halogenase subunits in a single polypeptide [16] or using cross-linked enzyme aggregates [11,29–32] can improve halogenation yield and enzyme stability.

In the more widely-studied two-component monooxygenase systems, a number of regulatory mechanisms have been described that regulate the reduction of flavin or promote the efficient shuttling of flavin between the two components [22]. The FR subunits typically have a higher affinity for the oxidized flavin than the reduced flavin, while the monooxygenase/halogenase subunits bind the reduced flavin more tightly [22]. Allosteric regulation by the substrate of the monooxygenase has been observed to affect flavin reduction as well as dissociation of reduced flavin from the FR in p-hydroxyphenylacetate hydroxylase [33]. Protein-protein interactions have been detected between the two subunits in several systems, and in some cases complex formation has been shown to regulate reduced flavin release or affect the kinetic parameters of the individual subunits [34–39]. The synergy observed in these two-component monooxygenase systems suggest that using a co-evolved halogenase/FR system, along with a detailed understanding of the kinetics and mechanism of flavin reduction, flavin transfer, and flavin utilization in that system, may be advantageous for optimizing *in vitro* halogenation reactions.

The biosynthetic gene clusters responsible for production of the cytotoxic indolotryptoline bisindole alkaloids BE-54017 and borregomycin A, which were discovered by metagenomic screening of soil samples from the Anza-Borrego desert, were predicted by sequence homology to each encode a two-component halogenase/FR system [40, 41]. BorF (Uniprot M9QXS1) is a flavin reductase that supplies the FADH₂ required by the tryptophan-6-halogenase BorH, which uses FADH₂ to convert water and chloride ion to HOCl, which in turn halogenates tryptophan in the initial steps of borregomycin biosynthesis

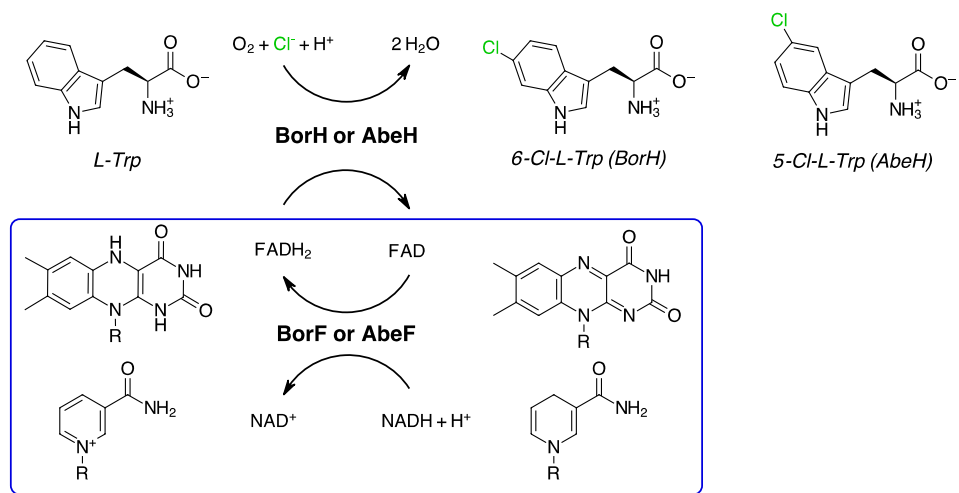
(Scheme 1) [41,42]. Likewise, AbeF and AbeH are products of the gene cluster responsible for BE-54017 biosynthesis, and sequence homology predicts AbeF (Uniprot F6LWA7) to be a flavin reductase and AbeH to be a tryptophan-5-halogenase [40]. BorF (196 residues) and AbeF (160 residues) share 30.57% sequence identity with one another. Understanding the detailed mechanisms of the catalytic cycles of the BorF/BorH and AbeF/AbeH two-component systems will provide a framework for determining optimal halogenation conditions by balancing flavin reduction by the FR with transfer to and utilization of reduced flavin by the halogenase. With this goal in mind, we have investigated the flavin reduction catalyzed by AbeF and BorF, determined substrate preferences, steady state kinetic parameters, and kinetic mechanisms, and identified some catalytically important residues.

2. Materials and methods

2.1. Protein expression and purification

An expression construct for His₆-MBP-BorF was previously cloned in our laboratory [43]. The construct was transformed into *E. coli* Rosetta2 (DE3)pLysS competent cells (EMD Biosciences), and the cells were cultured in LB Media (Research Products International) with 50 µg mL⁻¹ kanamycin and 30 µg mL⁻¹ chloramphenicol at 37 °C and 250 rpm until the OD₆₀₀ reached 0.8. The cells were induced by addition of 100 µM IPTG and grown for 20 h post induction at 16 °C and 250 rpm. Cells were harvested by centrifugation (4000×g for 40 min), resuspended in lysis buffer (20 mM Tris pH 7.5, 500 mM NaCl, 1 mM TCEP, 1 mM PMSF) and disrupted by sonication. The lysate was clarified by centrifugation (12,000×g for 20 min) and the clarified extract was applied to Co (II)-charged HisPur resin (Thermo Scientific). To remove bound FAD, the column was washed with 2 M urea and 2 M KBr [44]. Apo His₆-MBP-BorF protein was eluted using 20 mM Tris pH 7.5, 350 mM NaCl, 500 mM imidazole. PreScission protease was used to cleave the linker between His₆-MBP and BorF in an overnight digestion at 4 °C. The PreScission protease and cleaved His₆-MBP were removed from BorF by Co(II)-charged HisPur column, and the BorF was further purified by size exclusion chromatography using a HiLoad 10/300 Superdex 200 column equilibrated with 20 mM Tris pH 7.5, 100 mM NaCl. Holo-BorF (BorF with bound FAD) could be purified by the same procedure, omitting the 2 M urea/2 M KBr wash step.

To identify the source of the yellow color, holo-BorF was denatured by heating to 100 °C for 5 min, followed by removal of the precipitated protein by centrifugation at 16,000×g for 5 min. The yellow supernatant was analyzed by ESI-MS using a Thermo Finnigan LCQ Deca XP MS



Scheme 1. Reactions catalyzed by BorH/BorF and AbeH/AbeF. The halogenase subunit (BorH or AbeH) catalyzes the regioselective FADH₂-dependent chlorination of tryptophan, and the flavin reductase subunit (BorF or AbeF) catalyzes the reduction of FAD to FADH₂ using NADH (blue rectangle) [40–42].

System in negative ion mode.

A codon-optimized synthetic gene encoding AbeF (Thermo Fisher GeneArt) was amplified by polymerase chain reaction and ligated into vector pHIS_G28 using Gibson Assembly master mix (New England Biolabs) according to manufacturer's instructions. After sequencing verification, of the recombinant plasmid, encoding His₆-AbeF, was used to transform BL21 (DE3) expression hosts (New England Biolabs), and the cells were cultured in TB Media (Research Products International) with 50 µg mL⁻¹ kanamycin at 37 °C and 250 rpm until the OD₆₀₀ reached 0.8. The cells were induced by addition of 1 mM IPTG and grown for 18–20 h post induction at 16 °C and 250 rpm. Cells were harvested by centrifugation (4000×g for 40 min), resuspended in lysis buffer (20 mM Tris pH 7.5, 500 mM NaCl, 10 mM imidazole, 1 mM TCEP, 1 mM PMSF) and disrupted by sonication. The lysate was clarified by centrifugation (12,000×g for 20 min) and the clarified extract was applied to a Ni(II)-charged HisTrap column (GE Biosciences). Column-immobilized His-AbeF was stripped of FAD by washing with 2 M urea/2 M KBr, and the protein was eluted using 250 mM imidazole. Purified apo-AbeF was further purified by size exclusion chromatography on a Superdex S200 10/300 column in 20 mM HEPES pH 8.0, 150 mM NaCl.

Protein concentrations were measured using the Bradford assay (Bio-Rad Laboratories). FAD concentration was measured using 450 nm absorbance and the molar extinction coefficient of FAD (11,300 M⁻¹ cm⁻¹). NADH concentrations were measured using 340 nm absorbance and the molar extinction coefficient for NADH (6220 M⁻¹ cm⁻¹).

2.2. Flavin reductase activity assays

Flavin reductase activity was measured spectrophotometrically at 340 nm by monitoring the oxidation of NADH to NAD⁺. Absorbance measurements were recorded using a SpectraMax microplate reader (Molecular Devices). Initial velocities were calculated from slopes of the linear progress curves obtained. Assays were performed in 20 mM Tris pH 7.5 and were carried out at room temperature unless stated otherwise. Reaction volume was 200 µL and reactions were started by addition of apo-BorF or apo-AbeF to the reaction mixture.

To study substrate specificity of BorF, reactions were carried out with 25 µM FAD, FMN or riboflavin, 100 µM NADPH or NADH, and 60 nM apo-BorF. To study substrate specificity of AbeF, reactions were carried out with 20 µM FAD, FMN or riboflavin, 100 µM NADPH or NADH, and 50 nM apo-AbeF.

2.3. Steady state kinetic analysis

Steady state kinetic parameters were determined using the initial velocity method. Apo-BorF (60 nM) was reacted with variable concentrations of FAD (0.5–75 µM) at fixed concentrations of NADH (75, 125, 175, 225 µM), and with variable concentrations of NADH (10–225 µM) at fixed FAD concentrations (2, 10, 25, 50, 75 µM). Apo-AbeF (50 nM) was reacted with variable concentrations of FAD (0.25–25 µM) at fixed concentrations of NADH (10, 30, 50, 100 µM), and with variable concentrations of NADH (5–200 µM) at fixed FAD concentrations (2, 5, 10, 25 µM). The steady state kinetic parameters were obtained by nonlinear regression to fit the Michaelis-Menten equation (Eq. (1)). Double reciprocal plots (1/v₀ vs 1/[S]) were fit by linear regression. Curve fitting was done using Prism 8.0 (GraphPad, San Diego, California USA).

$$v_0 = \frac{V_{max}[S]}{K_M + [S]} \quad \text{Eq 1}$$

2.4. Inhibition studies

Product inhibition assays were conducted for apo-BorF and apo AbeF in the absence or presence of NAD⁺ using variable concentrations of either FAD or NADH at two different fixed concentrations of the other substrate. Similarly, dead end inhibition assays were performed in the

absence or presence of lumichrome using variable concentrations of either FAD or NADH with the second substrate held constant. Inhibitory constants (K_i) for competitive and mixed inhibition were calculated using Prism 8.0.

2.5. Site-directed mutagenesis

Site directed mutagenesis of BorF was carried out using the Q5 site directed mutagenesis kit (New England Biolabs) according to manufacturer's instructions using the primers in Table S7 to make the following BorF mutants: H160A, D159A, D159 N, and R38A.

2.6. pH rate profiling

pH rate profiles of wild type apo-AbeF and wild type, H160A, D159A, D159 N and R38A apo-BorF were analyzed by determining kinetic parameters for reactions performed in the following buffers (20 mM): sodium citrate (pH 5.0–5.5), Bis-Tris (pH 6.5), Tris-HCl (pH 7.5–8.5) and glycine (9.5). The values of k_{cat}/K_M against pH were then fit to a bell-shaped curve with Prism 8.0 using the kinetic expression for two ionizable groups (Equation (2) [45]) to determine apparent pK_a values.

$$\frac{k_{cat}}{K_M} = \frac{\left(\frac{k_{cat}}{K_M}\right)_{max}}{1 + 10^{(pK_a1-pH)} + 10^{(pH-pK_a2)}} \quad \text{Eq 2}$$

2.7. Measurement of dissociation constants

The binding of FAD, NADH, FADH₂ and lumichrome to apo-BorF and apo-AbeF was analyzed by protein fluorescence quenching titration measurements using a Quantmaster 40 fluorometer (Photon Technologies International) with excitation and emission wavelength of 285 and 333 nm respectively. FADH₂ was generated by treating FAD with 5 equivalents of sodium dithionite and storing under N₂. 100 nM of BorF in 20 mM Tris HCl pH 7.5 at 23 °C was titrated with increasing FAD (50 nM–2 µM), NADH (50 nM–30 µM), FADH₂ (100 nM–6 µM) and lumichrome (100 nM–6 µM). Binding of NADH to the BorF/lumichrome complex was determined by titrating 100 nM BorF and 20 µM lumichrome with increasing NADH (1–60 µM). Binding of ligands to AbeF was studied in the same manner by titrating FAD, lumichrome, FADH₂, and NADH into 100 nM apo-AbeF. Binding was analyzed by monitoring the decrease of the emission intensity due to the quenching of the protein fluorescence upon binding to ligand, as a function of titrant concentration and fitting the data to Equation (3) [46] ([B] = [protein], [A] = [ligand]) with Prism 8.0 to obtain the dissociation constant (K_D).

Binding of FAD and NADH to apo-BorF and to apo-AbeF were also investigated by fluorescence titration using the fluorescence of FAD and NADH. To measure FAD binding, FAD was excited at 450 nm and emission was measured at 525 nm using a Quantmaster 40 fluorometer (Photon Technologies International). 150 nM FAD in 20 mM Tris pH 7.5 at 23 °C was titrated with increasing BorF (50–2000 nM) to determine the K_D for FAD binding to BorF. Similarly, 100–2500 nM of AbeF was titrated into 150 nM FAD to determine the K_D for FAD binding to AbeF. To measure NADH binding, NADH was titrated with 0.5–15 µM BorF or 0.5–30 µM AbeF in 20 mM Tris pH 7.5 at 23 °C. NADH was excited at 340 nm and emission was measured at 450 nm. For these titrations, Equation (3) was used for calculation of the dissociation constants by substituting [ligand] for [B] and [protein] for [A].

$$\Delta F = \frac{\Delta F_{max}([A]_T + [B]_T + K_D) - \sqrt{[A]_T[B]_T[B]_T + K_D)^2 - 4[A]_T[B]_T}}{2[B]_T} \quad \text{Eq 3}$$

2.8. Phylogenetic analysis

BorF homologs were identified by a BLASTP search of non-redundant protein sequences in the NCBI database. Identified sequences with >20% sequence identity to BorF or AbeF and reported kinetic

mechanisms, kinetic parameters, or crystal structures were used to prepare a multiple sequence alignment using CLUSTAL Omega (EMBL-EBI) and formatted and annotated using ESPript 3.0 [47]. A phylogenetic tree was generated from the sequence alignment using MEGA X [48]. The bootstrap consensus tree was inferred from 500 replicates to represent the evolutionary history of the taxa analyzed using the Maximum Likelihood method and JTT matrix-based model.

3. Results and discussion

3.1. BorF and AbeF are NADH-dependent FRs with a preference for reducing FAD

BorF and AbeF were predicted to be FRs that reduce FAD to FADH_2 based on sequence homology with members of the short-chain FR family (Figure S1) and the discovery of their genes in gene clusters encoding two-component flavin-dependent halogenases. Despite the fact that both are components of biosynthetic pathways producing similar indolotryptoline natural products, phylogenetic analysis of short-chain FRs (Figure S2) places BorF and AbeF (which share 30% sequence identity with one another) in two different clades, with BorF most closely related to SgcE6, and AbeF most closely related to RebF.

BorF and AbeF were separately overexpressed in *E. coli* and purified to homogeneity using affinity chromatography and size exclusion chromatography (Figure S3). Other short-chain FRs supplying reduced flavin to two-component monooxygenase systems have been purified as yellow or colorless proteins depending on the amount of copurified flavin [21,49,50]. Fractions containing BorF and AbeF were yellow, indicating that they copurified with bound flavin. FAD was confirmed as the source of the yellow color by ESI-MS. FAD copurified with BorF and AbeF in substoichiometric molar ratios that varied from batch to batch, and could be completely removed from column-immobilized BorF or AbeF by washing with 2 M urea and 2 M KBr [44]. All of the assays described below were carried out using BorF and AbeF that were stripped of FAD using urea/KBr during purification (apo-BorF and apo-AbeF).

Purified BorF and AbeF could oxidize NADH in the presence of FAD, and the rate of NADH depletion was dependent on FR concentration (Figure S4). Relative activities of BorF and AbeF towards each possible combination of reductant (NADH and NADPH) and oxidized flavin (FAD, FMN and riboflavin) indicated that for both enzymes, FAD was the preferred substrate, and there was no activity with NADPH, which is common among the short-chain FRs (Figure S5). [21,51].

3.2. Steady-state kinetic analysis

Kinetic characterization of a number of short-chain FRs has identified a range of different mechanisms. FRs copurifying with a low amount of flavin, including ActVB [52], HpaC_{Tt} [53], SgcE6 [51], FerA [54], Tftc [55], StyB [56], and PrnF [57] have been shown to use sequential bi kinetic mechanisms, in which a hydride is transferred directly from NADH to FAD in a ternary complex. Of those, ActVB, HPaC_{Tt}, StyB and PrnF have been shown to use ordered sequential mechanisms, and FerA has been shown to use a random sequential mechanism.

In contrast, PheA2 [58] and TTHA0420 [59] use a ping-pong bi mechanism requiring a cofactor flavin as well as the substrate/product FAD. These FRs bind a molecule of FAD tightly as a prosthetic group and use a ping-pong bi kinetic mechanism, in which NADH transfers a hydride to reduce the cofactor FAD to FADH_2 , and then the cofactor FADH_2 reduces the substrate FAD to FADH_2 . This mechanism requires both a higher affinity for FAD in the conserved flavin binding site (which binds substrate/product flavin in FRs using a sequential mechanism and cofactor flavin in FRs using a ping-pong mechanism) and requires that the NADH binding site is able to accommodate both NADH and substrate FAD.

To investigate the kinetic mechanism of BorF and AbeF, the steady

state kinetic parameters for NADH oxidation were determined by the method of initial rates. Initial velocities for BorF were measured as a function of FAD concentration at fixed [NADH] (Fig. 1A) and as a function of NADH concentration at fixed [FAD] (Fig. 1B). Rates were fit to the Michaelis-Menten equation and steady state kinetic parameters of $K_M = 26.8 \mu\text{M}$ for NADH, $K_M = 1.3 \mu\text{M}$ for FAD, and turnover number (k_{cat}) = 56.5 s^{-1} were determined for BorF (Table 1). The higher K_M for NADH is typical for FRs [51]. Lineweaver-Burk plots of BorF initial velocities as a function of [FAD] at several fixed concentrations of NADH (Fig. 1C) and as a function of [NADH] at several fixed concentrations of FAD (Fig. 1D) intersected to the left of the ordinate, indicating a sequential kinetic mechanism involving a ternary complex.

For AbeF, initial velocity data fit to the Michaelis-Menten equation yielded kinetic constants of $K_M = 25.5 \mu\text{M}$ for NADH, $K_M = 1.5 \mu\text{M}$ for FAD, and $k_{\text{cat}} = 101.5 \text{ s}^{-1}$. (Fig. 2A and B, Table 1). Double reciprocal plots, of initial velocity dependence on [FAD] at fixed [NADH] and initial velocity dependence on [NADH] at fixed [FAD] also intersected to the left of the ordinate axis (Fig. 2C and D), indicating that AbeF also uses a sequential bi-bi mechanism for catalysis.

The K_M values for FAD and NADH obtained for BorF and AbeF are comparable with one another and with values determined for many other short-chain FRs and structurally related oxidoreductases (Table S1). AbeF's k_{cat} is 1.8 times higher than that of BorF, and both are within the range of reported values for members of this class, which ranges over several orders of magnitude from 2 s^{-1} to 200 s^{-1} (Table 1, Table S1).

3.3. Inhibition studies suggest different kinetic mechanisms for BorF and AbeF

Dead-end inhibition by lumichrome (7,8 dimethylalloxazine) was used to further probe the steady state kinetic mechanisms of BorF and AbeF. Lumichrome acts as a competitive inhibitor with respect to FAD for both enzymes (Fig. 3A, Fig. 5A, Table 2), ruling out an equilibrium sequential ordered mechanism, and a noncompetitive inhibitor with respect to NADH for both enzymes (Figs. 3B and 5B, Table 2), ruling out a Theorell-Chance kinetic mechanism. This suggested that BorF and AbeF have either steady state sequential ordered or sequential random kinetic mechanisms.

NAD^+ product inhibition data resolved this ambiguity. Our steady state kinetic data were collected with 0–5% of FAD converted to FADH_2 , so the effects of NAD^+ addition reflect product inhibition (formation of NAD^+/FAD dead end complexes) rather than a significant contribution of the endergonic reverse reaction (requiring $\text{NAD}^+/\text{FADH}_2$ complexes). NAD^+ acts as a competitive inhibitor of AbeF for both FAD and NADH at lower concentrations of fixed substrate (50 μM NADH and 5 μM FAD), meaning that FAD, NADH, and NAD^+ can all compete for binding to the same enzyme form (apo-AbeF), consistent with a rapid-equilibrium random sequential mechanism (Fig. 6A and B). The inhibition by NAD^+ is completely overcome by higher concentrations of either fixed substrate (200 μM NADH or 25 μM FAD), which is characteristic of a random sequential mechanism, since the excess substrate outcompetes the inhibitor for binding to the enzyme (Fig. 6 C and D and Table 2) [60]. In contrast, NAD^+ acted as a noncompetitive inhibitor of BorF with respect to both FAD and NADH (Fig. 4 and Table 3), which is consistent with NADH being the first product released in a steady state sequential ordered bi mechanism [60,61].

3.4. FAD binds BorF with higher affinity than AbeF, but NADH does not bind BorF in the absence of FAD

Since our kinetic data predicted that either substrate could bind first to AbeF but FAD was required to bind before NADH could bind to BorF, we carried out binding studies using fluorescence quenching to cross-validate our predicted kinetic mechanisms. Binding of FAD, NADH, FADH_2 , and lumichrome to apo-BorF and apo-AbeF was determined by

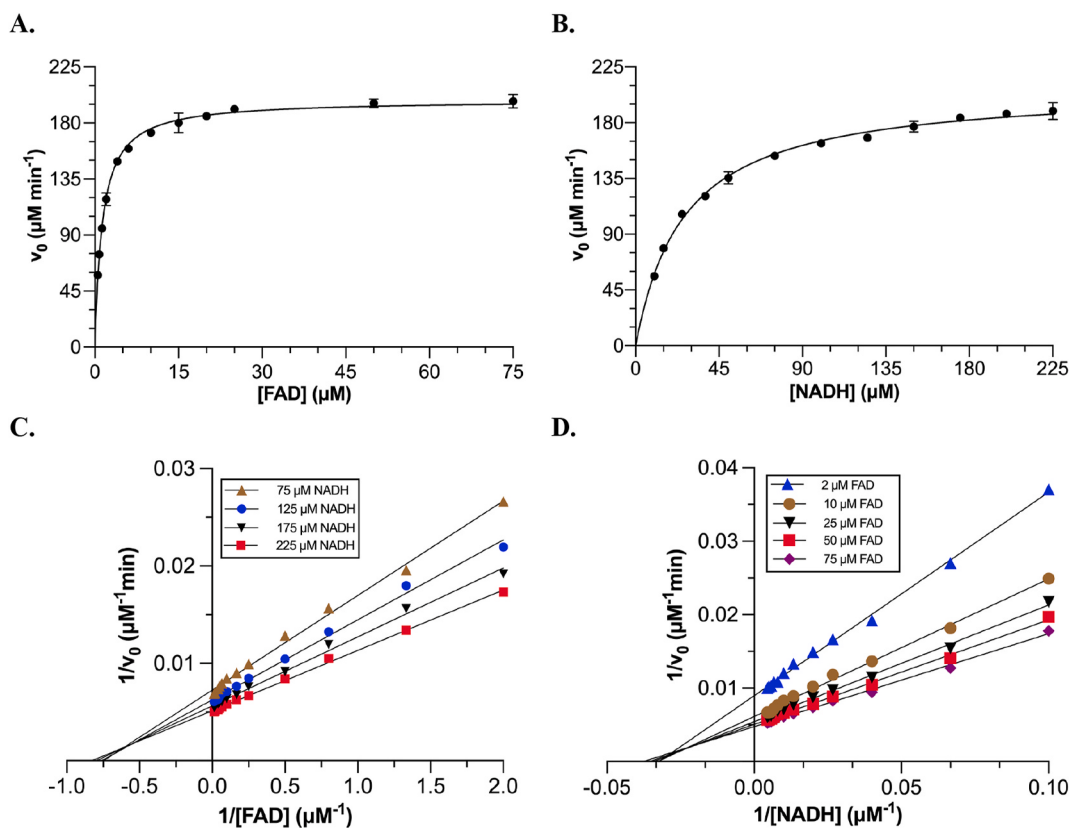


Fig. 1. Steady state kinetic analysis of BorF-catalyzed FAD reduction/NADH oxidation.

A. Initial velocities for reaction of 60 nM apo-BorF with 225 μ M NADH and 0.5–75 μ M FAD.

B. Initial velocities for reaction of 60 nM apo-BorF with 75 μ M FAD and 10–225 μ M NADH.

C. Double reciprocal (Lineweaver-Burk) plot of initial velocities as a function of FAD concentration for 60 nM apo-BorF in the presence of 75–225 μ M NADH.

D. Double reciprocal (Lineweaver-Burk) plot of initial velocities as a function of NADH concentration for 60 nM apo-BorF in the presence of 2–75 μ M FAD.

Table 1
Steady-state kinetic parameters for BorF and AbeF.

Enzyme	Variable substrate	Fixed substrate	K_m (μ M)	k_{cat} (s^{-1})
BorF	FAD	NADH	1.3 ± 0.1	55.1 ± 0.4
	NADH	FAD	27 ± 1	58.0 ± 0.7
	FMN	NADH	3.2 ± 0.5	49 ± 3
	Riboflavin	NADH	4.1 ± 0.7	44 ± 2
AbeF	FAD	NADPH	No activity	
	FAD	NADH	1.5 ± 0.2	100 ± 2
	NADH	FAD	26 ± 2	110 ± 2
	FMN	NADH	11 ± 2	71 ± 2
	Riboflavin	NADH	30 ± 10	47 ± 1
	FAD	NADPH	No activity	

titration using fluorescence quenching of the intrinsic tryptophan fluorescence of the proteins upon ligand binding (Figures S7–S17, Table 4). FAD bound to apo-AbeF with $K_D = 750$ nM, and FAD bound to apo-BorF with $K_D = 90$ nM (Figures S7, S12). The higher affinity of BorF for FAD is consistent with our observation that it required longer incubation times and more column volumes of 2 M urea/KBr to remove FAD from BorF compared to AbeF. Apo-AbeF bound the reduced product FADH₂ with $K_D = 1.5$ μ M, and the K_D for FADH₂ binding to apo-BorF was 780 nM (Figures S8, S13).

For apo-AbeF, binding could be observed for NADH in the absence of FAD ($K_D = 7.3$ μ M), consistent with a random kinetic mechanism in which either substrate can bind first (Figures S14, S19). In contrast, there was no change in either protein fluorescence or NADH fluorescence upon mixing apo-BorF with NADH, indicating that NADH does not bind to BorF in the absence of FAD (Figures S9, S19). This is consistent with an ordered mechanism in which FAD must bind before NADH.

NADH was able to bind BorF in the presence of lumichrome with $K_D = 29$ μ M, suggesting that the BorF-lumichrome complex was competent for binding NADH (Figure S11). The presence of lumichrome did not affect the K_D for NADH binding to AbeF (Figure S16), providing further support for a random sequential bi mechanism in which binding of one substrate does not affect the affinity for the other substrate.

The binding affinities of FAD and NADH to apo-BorF and apo-AbeF were independently measured by fluorescence titration using quenching of the intrinsic fluorescence of FAD ($\lambda_{em} = 525$ nm) and NADH ($\lambda_{em} = 450$ nm) upon binding to the protein (Figures S18 and S19), and the results were consistent with those obtained using protein fluorescence ($K_D = 110$ nM for BorF/FAD, $K_D = 740$ nM for AbeF/FAD, $K_D = 7.2$ μ M for AbeF/NADH, and no binding for BorF + NADH; Figure S18, S19).

The overall sequence conservation among the short-chain flavin reductases is fairly low (Figures S1 and S2), and there are few clues from sequence, phylogeny, or crystal structures to explain or predict the wide variation in binding affinities that have been reported as well as the array of diverse kinetic mechanisms. PheA2 has a substantially higher affinity for FAD than BorF or AbeF ($K_D = 10$ nM), and could not be stripped of flavin with 4 M urea [58,62]. This is consistent with the observation that PheA2 uses a two-flavin Ping-Pong mechanism in which the FAD binding site contains a tightly bound flavin cofactor and the substrate NADH and FAD alternate in the second binding site.

PrnF [57], ActVB [52], and StyB [56] have all been shown to use sequential ordered kinetic mechanisms, but unlike BorF, all three bind NADH first. PrnF has a K_D for FAD binding of 78 nM [39], 8 fold higher than PheA2 and comparable to BorF. FerA, which uses a random sequential kinetic mechanism like AbeF, has a K_D for FAD binding of 8.9 μ M and a K_D for NADH binding of 68 μ M [54], both of which are higher than the corresponding values for AbeF.

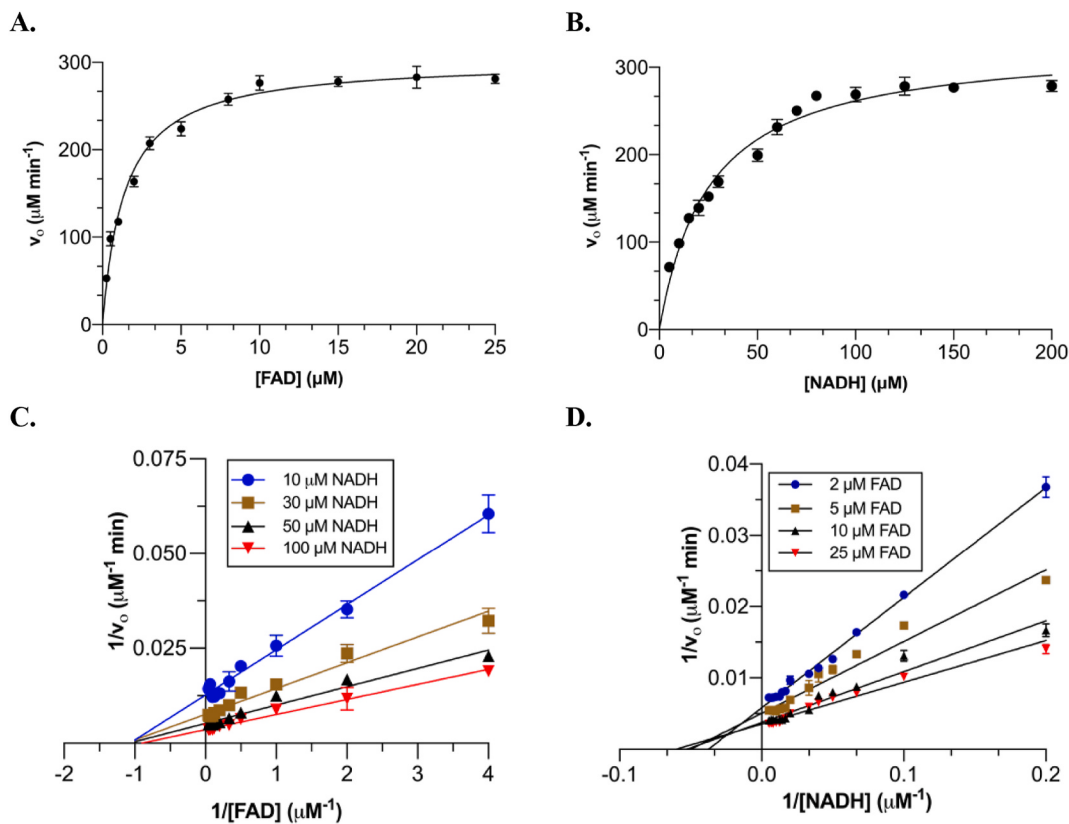


Fig. 2. Steady state kinetic analysis of AbeF-catalyzed FAD reduction/NADH oxidation.

A. Initial velocities for reaction of 50 nM apo-AbeF with 100 μM NADH and 0.25–25 μM FAD.
B. Initial velocities for reaction of 50 nM apo-AbeF with 25 μM FAD and 5–200 μM NADH.

C. Double reciprocal (Lineweaver-Burk) plot of initial velocities as a function of FAD concentration for 50 nM apo-AbeF in the presence of 10–100 μM NADH.
D. Double reciprocal (Lineweaver-Burk) plot of initial velocities as a function of NADH concentration for 50 nM apo-AbeF in the presence of 2–25 μM FAD.

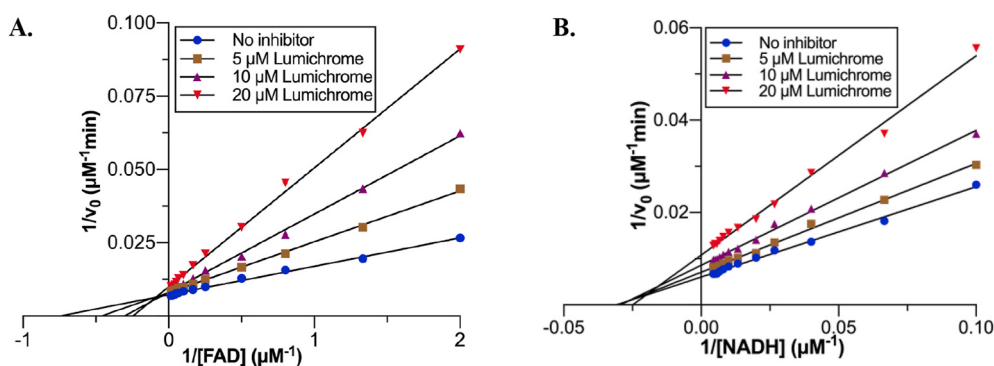


Fig. 3. Dead end inhibition of BorF activity by Lumichrome.

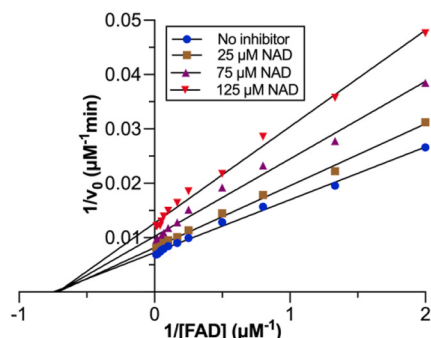
A. Double reciprocal (Lineweaver-Burk) plot of initial velocities as a function of FAD concentration for 60 nM apo-BorF and 75 μM NADH with 0–20 μM lumichrome.
B. Double reciprocal (Lineweaver-Burk) plot of initial velocities as a function of NADH concentration for 60 nM apo-BorF and 10 μM FAD with 0–20 μM lumichrome.

Table 2
Dead end inhibition by lumichrome.

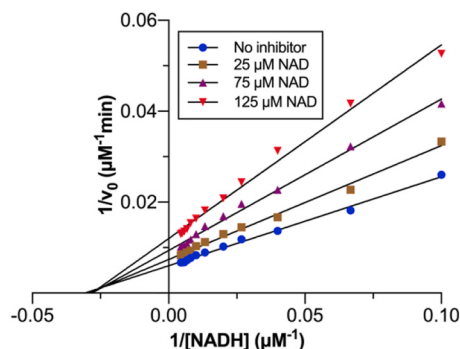
FR	Variable substrate	Fixed substrate	Mode of inhibition	K_i (μM)
BorF	FAD	NADH (75 μM)	Competitive	3.5 ± 0.6
	NADH	FAD (10 μM)	Noncompetitive	23 ± 1
AbeF	FAD	NADH (50 μM)	Competitive	6 ± 1
	NADH	FAD (5 μM)	Noncompetitive	22 ± 1

FRs from other two-component systems, such as FerA, HpaC, and ActVB, have been shown to bind oxidized flavin more tightly than the reduced form, while the monooxygenase binds reduced flavin with higher affinity, and this difference in affinity is thought to facilitate efficient flavin transfer [22,54]. BorF and AbeF both display this characteristic, binding FAD with higher affinity (2X and 8X respectively) than FADH₂.

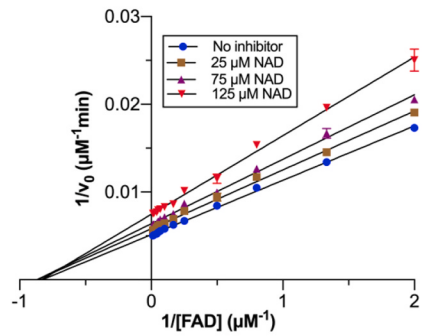
A.



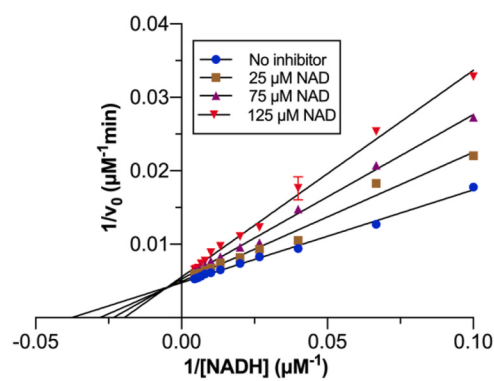
B.



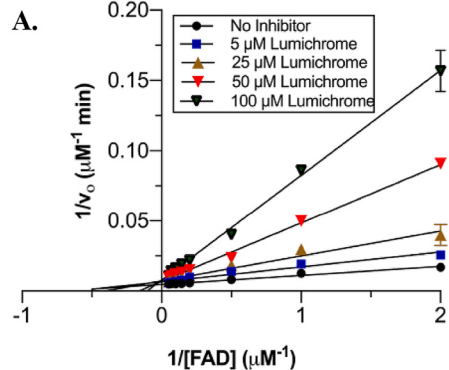
C.



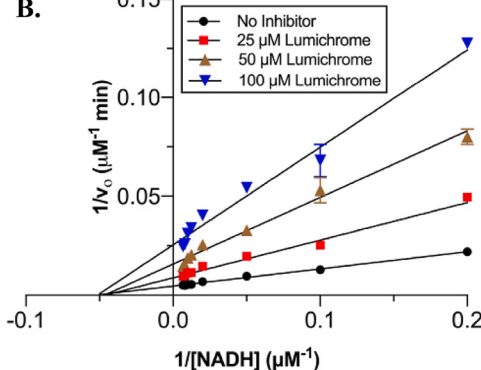
D.



A.



B.



3.5. BorF and AbeF activity is optimal at pH 7.5

To further probe the mechanism, the pH dependence of BorF's k_{cat} was determined and found to produce a bell-shaped curve with a maximum at pH 7.5 (Fig. 7). The BorF pH rate profile indicated that functional groups with pK_a values of approximately 5.9 and 9.3 are important for activity. BorF's K_M for FAD varied little over the entire pH range, and the K_M for NADH was unchanged above pH 6.0; however, the k_{cat} at the endpoints of the pH range was only about half of the k_{cat} at pH 7.5 (Tables S2 and S3). The pH dependence of k_{cat} and K_M for AbeF showed the same trend (Figure S20 and Table S4).

Based on the pH rate profile and sequence homology, we hypothesized that the loss of activity at pH < 7.5 corresponding to pK_a 5.9 may be attributed to protonation of His160, and the loss of activity above pH 7.5 corresponding to pK_a 9.3 may be attributed to deprotonation of Arg38. His160 is one of only three residues absolutely conserved among short-chain FRs (Figure S1) and is a part of a conserved GDH motif in the

NADH binding site that forms a hydrogen bond with the nicotinamide amide group [54,63] (Figure S21). Arg38 is also conserved, and can be seen in the PheA2/FAD/NAD crystal structure interacting with the phosphoanhydride of NAD⁺ [58] (Figure S21). These residues are also conserved in AbeF (His127 and Arg8).

We mutated His160 and Arg38 to alanine in BorF to test the contributions of these residues to catalytic activity and pH dependence. We also mutated Asp159 which is part of the GDH motif implicated in substrate binding to both A and N. The purified mutants (H160A, R38A, D159A, and D159 N) all copurified with FAD, eluted as dimers on size exclusion chromatography, and showed FR activity (Figure S3A, Fig. 7, Table 4). D159 N has a k_{cat} close to that of wild type BorF, and D159A shows reduced catalytic activity, suggesting that D159 plays a role that does not require negative charge or acid-base catalysis. Both D159 mutants showed the same pH dependence as wild type BorF. R38A has a greater than twofold decrease in k_{cat} at pH 7.5, which decreases further below but not above pH 7.5. H160A has 10-fold reduced activity, which

Fig. 4. Product inhibition of BorF activity by NAD⁺.

A. Double reciprocal (Lineweaver-Burk) plot of initial velocities as a function of FAD concentration for 60 nM apo-BorF and 75 μM NADH with 0–125 μM NAD⁺.

B. Double reciprocal (Lineweaver-Burk) plot of initial velocities as a function of NADH concentration for 60 nM apo-BorF and 10 μM FAD with 0–125 μM NAD⁺.

C. Double reciprocal (Lineweaver-Burk) plot of initial velocities as a function of FAD concentration for 60 nM apo-BorF and 225 μM NADH with 0–125 μM NAD⁺.

D. Double reciprocal (Lineweaver-Burk) plot of initial velocities as a function of NADH concentration for 60 nM apo-BorF and 75 μM FAD with 0–125 μM NAD⁺.

Fig. 5. Dead end inhibition of AbeF activity by Lumichrome.

A. Double reciprocal (Lineweaver-Burk) plot of initial velocities as a function of FAD concentration for 50 nM apo-AbeF and 50 μM NADH with 0–100 μM lumichrome.

B. Double reciprocal (Lineweaver-Burk) plot of initial velocities as a function of NADH concentration for 50 nM apo-AbeF and 5 μM FAD with 0–100 μM lumichrome.

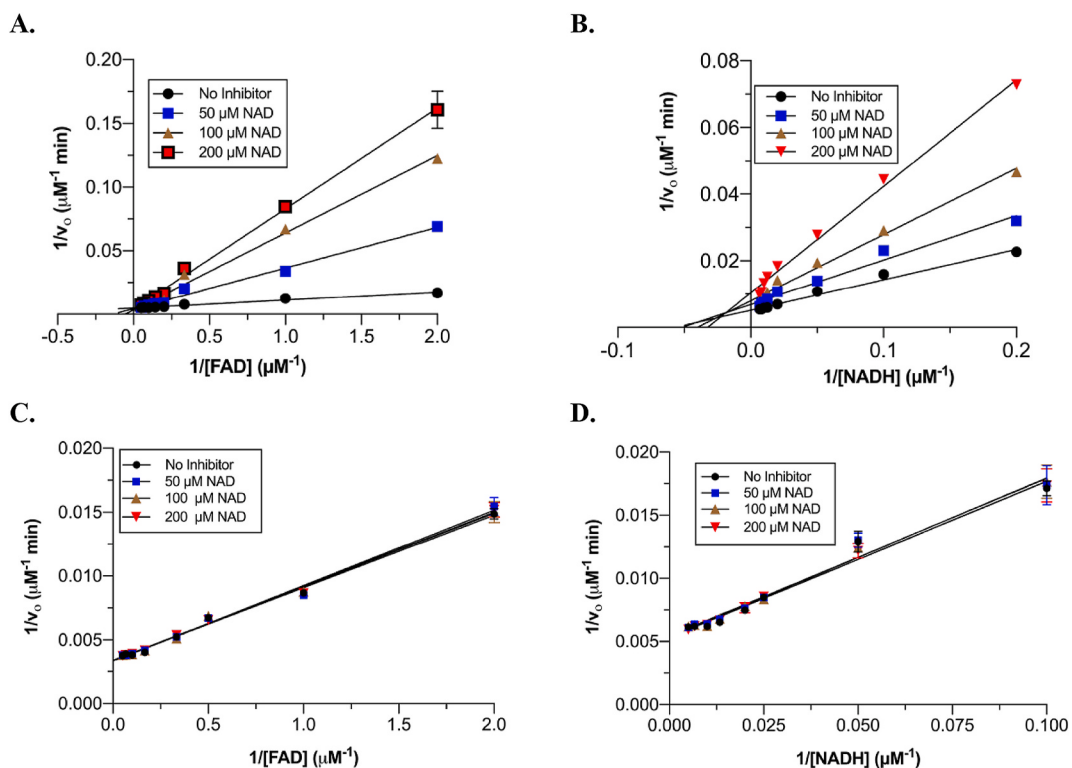


Fig. 6. Product inhibition of AbeF activity by NAD⁺.

A. Double reciprocal (Lineweaver-Burk) plot of initial velocities as a function of FAD concentration for 50 nM apo-AbeF and 50 μM NADH with 0–200 μM NAD⁺.

B. Double reciprocal (Lineweaver-Burk) plot of initial velocities as a function of NADH concentration for 50 nM apo-AbeF and 5 μM FAD 0–200 μM NAD⁺.

C. Double reciprocal (Lineweaver-Burk) plot of initial velocities as a function of FAD concentration for 50 nM apo-AbeF and 200 μM NADH with 0–200 μM NAD⁺.

D. Double reciprocal (Lineweaver-Burk) plot of initial velocities as a function of NADH concentration for 50 nM apo-AbeF and 25 μM FAD with 0–200 μM NAD⁺.

Table 3
Product inhibition by NAD⁺.

FR	Variable substrate	Fixed substrate	Mode of inhibition	K_i (μM)
AbeF	FAD	NADH (75 μM)	Noncompetitive	200 ± 10
	NADH	FAD (10 μM)	Noncompetitive	131 ± 6
	FAD	NADH (225 μM)	Noncompetitive	290 ± 10
	NADH	FAD (75 μM)	Noncompetitive	69 ± 6
	FAD	NADH (50 μM)	Competitive	26 ± 5
	NADH	FAD (5 μM)	Competitive	41 ± 9
	FAD	NADH (200 μM)	No inhibition	
	NADH	FAD (25 μM)	No inhibition	

Table 4

Dissociation constants measured from fluorescence titration. K_D values were determined from protein intrinsic tryptophan fluorescence except for ^a (determined using FAD fluorescence) and ^b (determined using NADH fluorescence).

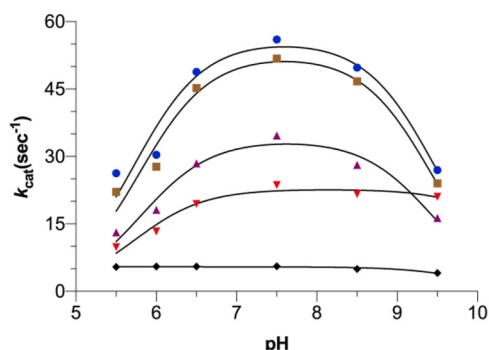
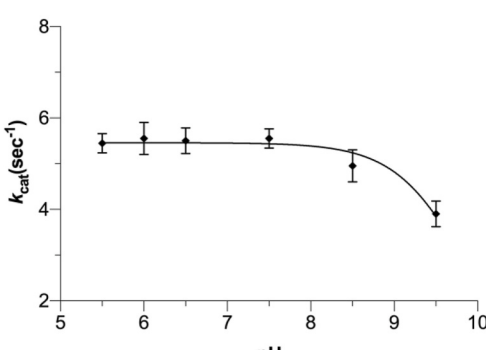
Ligand	Protein or complex	K_D
FAD	Apo-AbeF	750 ± 20 nM
	Apo-BorF	740 ± 10 nM ^a
FADH ₂	Apo-AbeF	91 ± 4 nM
	Apo-BorF	112 ± 3 nM ^a
Lumichrome	Apo-AbeF	1510 ± 20 nM
	Apo-BorF	800 ± 200 nM
NADH	Apo-AbeF	810 ± 30 nM
	AbeF/NADH	800 ± 20 nM
	Apo-BorF	1.9 ± 0.5 mM
	BorF/NADH	Not determined
AbeF/Lumichrome	Apo-AbeF	7.3 ± 0.1 mM
	AbeF/Lumichrome	7.5 ± 0.3 mM
	Apo-BorF	No binding observed
	BorF/Lumichrome	29 ± 7 mM

decreases further above but not below pH 7.5 (Fig. 7 and Table 5). Taken together, these data suggest a requirement for deprotonated His160 and protonated Arg38 for optimal activity. These residues have been implicated in NADH binding, and this is reflected in a small increase in the K_M for NADH for H160A and R38A, but no significant changes for D159A or D159 N. The K_M for FAD was slightly elevated in all four mutants.

The corresponding residues (His 146 and Arg 29) were previously mutated in FerA, and those mutations had a more drastic effect on FerA activity. Both H146A and R29A FerA mutants only retained about 3% of the activity of wild type FerA. H146A FerA had no change in the K_M for FMN, and a small increase in the K_M for NADH, while R29A FerA had decreased K_M values for both substrates [54].

4. Conclusions

BorF and AbeF are both short-chain flavin reductases providing FADH₂ to tryptophan halogenases in two biosynthetic pathways producing indolotryptoline natural products in soil bacteria. Both are selective for NADH over NADPH and prefer FAD as a substrate but are able to reduce FMN and riboflavin as well. AbeF has a k_{cat} approximately twice that of BorF, and uses a random sequential kinetic mechanism, whereas BorF uses an ordered sequential mechanism with FAD as the leading substrate, a model reinforced by the inability of BorF to bind NADH in the absence of FAD. Both AbeF and BorF, bind FAD with higher affinity than FADH₂, which likely helps to favor the efficient cycling of flavin between the FR and halogenase subunits. Further exploration of the structural features that lead to the diversity in flavin affinity and kinetic mechanism, as well as potential interactions with the halogenase subunits as have been described for two component monooxygenases, will be valuable in the further development of BorH, AbeH, and other halogenases as biocatalysts.

A.**B.****Fig. 7.** pH dependence of k_{cat} for wild type and mutant BorF.

A. pH dependence of k_{cat} for 60 nM wild type BorF (blue circles) and 100 nM BorF mutants D159 N (brown squares) D159A (purple triangles) R38A (red triangles), and H160A (black diamonds) at fixed 225 μ M NADH and 0.5–20 μ M variable FAD. Optimal activity for wild type BorF is at pH 7.5. D159 N has 93% activity compared to wild type BorF, and that activity drops to 60% for D159A, but both D159 mutants show the same pH dependence as wild-type. R38A has 40% activity, which decreases further below pH 7.5 but not above 7.5. H160A has the greatest reduction in activity (10% of wild type), which decreases further above pH 7.5

but not below 7.5.

B. Magnification of k_{cat} vs. pH for BorF H160A showing the further decrease in activity above pH 7.5. (For interpretation of the references to color in this figure legend, the reader is referred to the Web version of this article.)

Table 5

Steady-state kinetic parameters of BorF mutants.

Enzyme	k_{cat} (s^{-1})	K_M FAD (μ M)	K_M NADH (μ M)
Wild Type	57 ± 2	1.3 ± 0.1	27 ± 1
H160A	5.6 ± 0.5	1.7 ± 0.4	44 ± 2
D159A	34 ± 3	1.8 ± 0.5	30 ± 2
D159 N	53 ± 2	1.8 ± 0.3	27 ± 1
R38A	22 ± 2	1.9 ± 0.5	37 ± 1

Author contributions

AJDS was responsible for experimental design, BorF purification, kinetic analysis, fluorescence and mutagenesis experiments, sequence alignment and phylogenetic analysis, data interpretation, manuscript writing and editing, and figure preparation. RS was responsible for experimental design, AbeF purification, kinetic analysis, and fluorescence experiments, data interpretation, manuscript writing and editing, and figure preparation. JK was responsible for cloning and expression of AbeF. JJB was responsible for experimental design, data interpretation, manuscript writing and editing, and figure preparation. All authors have given approval to the final version of the manuscript.

Funding sources

This work was supported by National Institutes of Health Grant R15 GM110679-01A1 and an award from the University of Toledo Research Awards and Fellowship Program (I-128219-01).

Appendix A. Supplementary data

Supplementary data to this article can be found online at <https://doi.org/10.1016/j.abb.2021.108874>.

References

- J. Büchler, A. Papadopoulou, R. Buller, Recent advances in flavin-dependent halogenase biocatalysis: sourcing, engineering, and application, *Catalysts* 9 (2019), <https://doi.org/10.3390/catal9121030>, 1030–1020.
- P. Chenprakhon, T. Wongnate, P. Chaiyen, Monooxygenation of aromatic compounds by flavin-dependent monooxygenases, *Protein Sci.* 28 (2018) 8–29, <https://doi.org/10.1002/pro.3525>.
- M.M.E. Huijbers, S. Montersino, A.H. Westphal, D. Tischler, W.J.H. van Berkel, Flavin dependent monooxygenases, *Arch. Biochem. Biophys.* 544 (2014) 2–17, <https://doi.org/10.1016/j.abb.2013.12.005>.
- S. Nijvipakul, D.P. Ballou, P. Chaiyen, Reduction kinetics of a flavin oxidoreductase LuxG from *Photobacterium leiognathi* (TH1): half-sites reactivity, *Biochemistry* 49 (2010) 9241–9248, <https://doi.org/10.1021/bi1009985>.
- T. Heine, W. van Berkel, G. Gassner, K.-H. van Pee, D. Tischler, Two-component FAD-dependent monooxygenases: current knowledge and biotechnological opportunities, *Biology* 7 (2018), <https://doi.org/10.3390/biology7030042>, 42–35.
- H.R. Ellis, The FMN-dependent two-component monooxygenase systems, *Arch. Biochem. Biophys.* 497 (2010) 1–12, <https://doi.org/10.1016/j.abb.2010.02.007>.
- S.C. Tu, Reduced flavin: donor and acceptor enzymes and mechanisms of channeling, *Antioxid. Redox Signaling* 3 (2001) 881–897, <https://doi.org/10.1089/15230860152665046>.
- V. Sedlacek, I. Kucera, Functional and mechanistic characterization of an atypical flavin reductase encoded by the pden_5119 gene in *Paracoccus denitrificans*, *Mol. Microbiol.* 112 (2019) 166–183, <https://doi.org/10.1111/mmi.14260>.
- A.E. Fraley, D.H. Sherman, Halogenase engineering and its utility in medicinal chemistry, *Bioorg. Med. Chem. Lett* 28 (2018) 1992–1999, <https://doi.org/10.1016/j.bmcl.2018.04.066>.
- J. Latham, E. Brandenburger, S.A. Shepherd, B.R.K. Menon, J. Micklefield, Development of halogenase enzymes for use in synthesis, *Chem. Rev.* 118 (2018) 232–269, <https://doi.org/10.1021/acscchemrev.7b00032>.
- M. Frese, N. Sewald, Enzymatic halogenation of tryptophan on a gram scale, *Angew. Chem. Int. Ed. Engl.* 54 (2015) 298–301, <https://doi.org/10.1002/anie.201408561>.
- B.R.K. Menon, E. Brandenburger, H.H. Sharif, U. Klemstein, S.A. Shepherd, M. F. Greaney, J. Micklefield, RadH, A versatile halogenase for integration into synthetic pathways, *Angew. Chem. Int. Ed. Engl.* 56 (2017) 11841–11845, <https://doi.org/10.1002/anie.201706342>.
- B.R.K. Menon, D. Richmond, N. Menon, Halogenases for biosynthetic pathway engineering: toward new routes to naturals and non-naturals, *Catal. Rev.* (2020) 1–59, <https://doi.org/10.1080/01614940.2020.1823788>, 00.
- J.T. Payne, M.C. Andorfer, J.C. Lewis, Regioselective arene halogenation using the FAD-dependent halogenase RebH, *Angew. Chem. Int. Ed. Engl.* 52 (2013) 5271–5274, <https://doi.org/10.1002/anie.201300762>.
- D.R.M. Smith, S. Grützschow, R.J.M. Goss, Scope and potential of halogenases in biosynthetic applications, *Curr. Opin. Chem. Biol.* 17 (2013) 276–283, <https://doi.org/10.1016/j.cbpa.2013.01.018>.
- M.C. Andorfer, K.D. Belsare, A.M. Girlich, J.C. Lewis, Aromatic halogenation by using bifunctional flavin reductase-halogenase fusion enzymes, *Chembiochem* 18 (2017) 2099–2103, <https://doi.org/10.1002/cbic.201700391>.
- M.C. Andorfer, J.C. Lewis, Understanding and improving the activity of flavin-dependent halogenases via random and targeted mutagenesis, *Annu. Rev. Biochem.* 87 (2018) 159–185, <https://doi.org/10.1146/annurev-biochem-062917-012042>.
- S. Brown, S.E. O'Connor, Halogenase engineering for the generation of new natural product analogues, *Chembiochem* 16 (2015) 2129–2135, <https://doi.org/10.1002/cbic.201500338>.
- W.S. Glenn, E. Nims, S.E. O'Connor, Reengineering a tryptophan halogenase to preferentially chlorinate a direct alkaloid precursor, *J. Am. Chem. Soc.* 133 (2011) 19346–19349, <https://doi.org/10.1021/ja2089348>.
- C.B. Poor, M.C. Andorfer, J.C. Lewis, Improving the stability and catalyst lifetime of the halogenase RebH by directed evolution, *Chembiochem* 15 (2014) 1286–1289, <https://doi.org/10.1002/cbic.201300780>.
- B. Galan, E. Diaz, M.A. Prieto, J.L. Garcia, Functional analysis of the small component of the 4-hydroxyphenylacetate 3-monooxygenase of *Escherichia coli* W: a prototype of a new Flavin:NAD(P)H reductase subfamily, *J. Bacteriol.* 182 (2000) 627–636, <https://doi.org/10.1128/jb.182.3.627-636.2000>.

- [22] J. Sucharitakul, R. Tinikul, P. Chaiyen, Mechanisms of reduced flavin transfer in the two-component flavin-dependent monooxygenases, *Arch. Biochem. Biophys.* 555–556 (2014) 33–46, <https://doi.org/10.1016/j.abb.2014.05.009>.
- [23] C. Seibold, H. Schnerr, J. Rumpf, A. Kunzendorf, C. Hatscher, T. Wage, A.J. Ernyei, C. Dong, J.H. Naismith, K.-H. van Pee, A flavin-dependent tryptophan 6-halogenase and its use in modification of pyrrolinitrin biosynthesis, *Biocatal. Biotransform.* 24 (2006) 401–408, <https://doi.org/10.1080/10242420601033738>.
- [24] J. Zeng, A.K. Lytle, D. Gage, S.J. Johnson, J. Zhan, Specific chlorination of isoquinolines by a fungal flavin-dependent halogenase, *Bioorg. Med. Chem. Lett.* 23 (2013) 1001–1003, <https://doi.org/10.1016/j.bmcl.2012.12.038>.
- [25] J. Zeng, J. Zhan, Characterization of a tryptophan 6-halogenase from *Streptomyces toxytricini*, *Biotechnol. Lett.* 33 (2011) 1607–1613, <https://doi.org/10.1007/s10529-011-0595-7>.
- [26] B.R.K. Menon, E. Brandenburger, H.H. Sharif, U. Klemstein, S.A. Shepherd, M. F. Greaney, J. Micklefield, RadH, A versatile halogenase for integration into synthetic pathways, *Angew. Chem.* 56 (2017) 11841–11845, <https://doi.org/10.1002/anie.201706342>.
- [27] J. Lee, J. Kim, H. Kim, E.J. Kim, H.J. Jeong, K.-Y. Choi, B.G. Kim, Characterization of a tryptophan 6-halogenase from *Streptomyces albus* and its regioselectivity determinants, *Chembiochem* 21 (2020) 1446–1452, <https://doi.org/10.1002/cbic.201900723>.
- [28] A. Phintha, K. Prakinee, A. Jaruwat, N. Lawan, S. Visitsatthawong, C. Kantiwiriyawanitch, W. Songsungthong, D. Trisrirat, P. Chenprakhon, A. Mulholland, K.-H. van Pee, P. Chitnumsub, P. Chaiyen, Dissecting the low catalytic capability of flavin-dependent halogenases, *J. Biol. Chem.* 296 (2020), 100068, <https://doi.org/10.1074/jbc.RA120.016004>.
- [29] M. Frese, C. Schnebel, H. Minges, H. Voß, R. Feiner, N. Sewald, Modular combination of enzymatic halogenation of tryptophan with suzuki-miyaura cross-coupling reactions, *ChemCatChem* 8 (2016) 1799–1803, <https://doi.org/10.1002/cctc.201600317>.
- [30] J. Latham, J.-M. Henry, H.H. Sharif, B.R.K. Menon, S.A. Shepherd, M.F. Greaney, J. Micklefield, Integrated catalysis opens new arylation pathways via regiodivergent enzymatic C-H activation, *Nat. Commun.* 7 (2016) 11873, <https://doi.org/10.1038/ncomms11873>.
- [31] C. Schnebel, H. Minges, M. Frese, N. Sewald, A high-throughput fluorescence assay to determine the activity of tryptophan halogenases, *Angew. Chem. Int. Ed. Engl.* 55 (2016) 14159–14163, <https://doi.org/10.1002/anie.201605635>.
- [32] S.A. Shepherd, B.R.K. Menon, H. Fisk, A.-W. Struck, C. Levy, D. Ley, J. Micklefield, A structure-guided switch in the regioselectivity of a tryptophan halogenase, *Chembiochem* 17 (2016) 821–824, <https://doi.org/10.1002/cbic.201600051>.
- [33] J. Sucharitakul, T. Phongsak, B. Entsch, J. Svasti, P. Chaiyen, D.P. Ballou, Kinetics of a two-component p-hydroxyphenylacetate hydroxylase explain how reduced flavin is transferred from the reductase to the oxygenase, *Biochemistry* 46 (2007) 8611–8623, <https://doi.org/10.1021/bi7006614>.
- [34] C.E. Jeffers, J.C. Nichols, S.-C. Tu, Complex formation between *Vibrio harveyi* luciferase and monomeric NADPH:FMN oxidoreductase, *Biochemistry* 42 (2003) 529–534, <https://doi.org/10.1021/bi026877n>.
- [35] K. Abdurachim, H.R. Ellis, Detection of protein-protein interactions in the alkanesulfonate monooxygenase system from *Escherichia coli*, *J. Bacteriol.* 188 (2006) 8153–8159, <https://doi.org/10.1128/JB.00966-06>.
- [36] S. Nijvipakul, J. Wongratana, C. Suadee, B. Entsch, D.P. Ballou, P. Chaiyen, LuxG is a functioning flavin reductase for bacterial luminescence, *J. Bacteriol.* 190 (2008) 1531–1538, <https://doi.org/10.1128/JB.01660-07>.
- [37] S. Chakraborty, M. Ortiz-Maldonado, B. Entsch, D.P. Ballou, Studies on the mechanism of p-hydroxyphenylacetate 3-hydroxylase from *Pseudomonas aeruginosa*: a system composed of a small flavin reductase and a large flavin-dependent oxygenase, *Biochemistry* 49 (2010) 372–385, <https://doi.org/10.1021/bi901454u>.
- [38] E. Morrison, A. Kantz, G.T. Gassner, M.H. Sazinsky, Structure and mechanism of styrene monooxygenase reductase: new insight into the FAD-transfer reaction, *Biochemistry* 52 (2013) 6063–6075, <https://doi.org/10.1021/bi0400763n>.
- [39] J.K. Lee, H. Zhao, Identification and characterization of the flavin:NADH reductase (PmfF) involved in a novel two-component arylamine oxygenase, *J. Bacteriol.* 189 (2007) 8556–8563, <https://doi.org/10.1128/JB.01050-07>.
- [40] F.-Y. Chang, S.F. Brady, Cloning and characterization of an environmental DNA-derived gene cluster that encodes the biosynthesis of the antitumor substance BE-54017, *J. Am. Chem. Soc.* 133 (2011) 9996–9999, <https://doi.org/10.1021/ja2022653>.
- [41] F.Y. Chang, S.F. Brady, Discovery of indolotryptoline antiproliferative agents by homology-guided metagenomic screening, *Proc. Natl. Acad. Sci. U.S.A.* 110 (2013) 2478–2483, <https://doi.org/10.1073/pnas.1218073110>.
- [42] K. Lingkon, J.J. Bellizzi, Structure and activity of the thermophilic tryptophan-6-halogenase BorH, *Chembiochem* 21 (2020) 1121–1128, <https://doi.org/10.1002/cbic.201900667>.
- [43] Z. Ma, *Biochemical and Structural Studies of CLOCK, BMAL1, Nocturnin and BorF, Chemistry and Biochemistry, University of Toledo, Toledo, OH, 2015*.
- [44] M.H. Hefti, F.J. Milder, S. Boeren, J. Vervoort, W.J.H. van Berkel, A His-tag based immobilization method for the preparation and reconstitution of apoflavoproteins, *Biochim. Biophys. Acta Gen. Subj.* 1619 (2003) 139–143, [https://doi.org/10.1016/s0304-4165\(02\)00474-9](https://doi.org/10.1016/s0304-4165(02)00474-9).
- [45] N. Timms, C.L. Windle, A. Polyakova, J.R. Ault, C.H. Trinh, A.R. Pearson, A. Nelson, A. Berry, Structural insights into the recovery of aldolase activity in N-acetylneuraminate acid lyase by replacement of the catalytically active lysine with gamma-thialysine by using a chemical mutagenesis strategy, *Chembiochem* 14 (2013) 474–481, <https://doi.org/10.1002/cbic.201200714>.
- [46] K.A. Bakar, S.R. Feroz, A critical view on the analysis of fluorescence quenching data for determining ligand-protein binding affinity, *Spectrochim. Acta, Part A* 223 (2019), 117337, <https://doi.org/10.1016/j.saa.2019.117337>.
- [47] X. Robert, P. Gouet, Deciphering key features in protein structures with the new ENDscript server, *Nucleic Acids Res.* 42 (2014) W320–W324, <https://doi.org/10.1093/nar/gku316>.
- [48] G. Stecher, K. Tamura, S. Kumar, Molecular evolutionary genetics analysis (MEGA) for macOS, *Mol. Biol. Evol.* 37 (2020) 1237–1239, <https://doi.org/10.1093/molbev/msz312>.
- [49] T.M. Louie, H. Yang, P. Karnchanaphanurach, X.S. Xie, L. Xun, FAD is a preferred substrate and an inhibitor of *Escherichia coli* general NAD(P)H:flavin oxidoreductase, *J. Biol. Chem.* 277 (2002) 39450–39455, <https://doi.org/10.1074/jbc.M206339200>.
- [50] P. Chaiyen, C. Suadee, P. Wilairat, A novel two-protein component flavoprotein hydroxylase, *Eur. J. Biochem.* 268 (2001) 5550–5561, <https://doi.org/10.1046/j.1432-1033.2001.02490.x>.
- [51] S.G. Van Lanen, S. Lin, G.P. Horsman, B. Shen, Characterization of SgcE6, the flavin reductase component supporting FAD-dependent halogenation and hydroxylation in the biosynthesis of the enediyne antitumor antibiotic C-1027, *FEMS Microbiol. Lett.* 300 (2009) 237–241, <https://doi.org/10.1111/j.1574-6968.2009.01802.x>.
- [52] L. Filisetti, M. Fontecave, V. Niviere, Mechanism and substrate specificity of the flavin reductase ActVB from *Streptomyces coelicolor*, *J. Biol. Chem.* 278 (2003) 296–303, <https://doi.org/10.1074/jbc.M209689200>.
- [53] S.H. Kim, T. Hisano, W. Iwasaki, A. Ebihara, K. Miki, Crystal structure of the flavin reductase component (HpaC) of 4-hydroxyphenylacetate 3-monooxygenase from *Thermus thermophilus* HB8: structural basis for the flavin affinity, *Proteins: Struct., Funct., Bioinf.* 70 (2008) 718–730, <https://doi.org/10.1002/prot.21534>.
- [54] V. Sedlacek, T. Klumpler, J. Marek, I. Kucera, Biochemical properties and crystal structure of the flavin reductase FerA from *Paracoccus denitrificans*, *Microbiol. Res.* 188–189 (2016) 9–22, <https://doi.org/10.1016/j.micres.2016.04.006>.
- [55] M.R. Gisi, L. Xun, Characterization of chlorophenol 4-monooxygenase (TftD) and NADH:flavin adenine dinucleotide oxidoreductase (TftC) of *Burkholderia cepacia* AC1100, *J. Bacteriol.* 185 (2003) 2786–2792, <https://doi.org/10.1128/jb.185.9.2786-2792.2003>.
- [56] K. Otto, K. Hofstetter, M. Rothlisberger, B. Witholt, A. Schmid, Biochemical characterization of StyAB from *Pseudomonas* sp. strain VLB120 as a two-component flavin-diffusible monooxygenase, *J. Bacteriol.* 186 (2004) 5292–5302, <https://doi.org/10.1128/JB.186.16.5292-5302.2004>.
- [57] M.K. Tiwari, R.K. Singh, J.K. Lee, H. Zhao, Mechanistic studies on the flavin:NADH reductase (PrnF) from *Pseudomonas fluorescens* involved in arylamine oxygenation, *Bioorg. Med. Chem. Lett.* 22 (2012) 1344–1347, <https://doi.org/10.1016/j.bmcl.2011.12.078>.
- [58] R.H. van den Heuvel, A.H. Westphal, A.J. Heck, M.A. Walsh, S. Rovida, W.J. van Berkel, A. Mattevi, Structural studies on flavin reductase PheA2 reveal binding of NAD in an unusual folded conformation and support novel mechanism of action, *J. Biol. Chem.* 279 (2004) 12860–12867, <https://doi.org/10.1074/jbc.M313765200>.
- [59] T. Imagawa, T. Tsurumura, Y. Sugimoto, K. Aki, K. Ishidoh, S. Kuramitsu, H. Tsuge, Structural basis of free reduced flavin generation by flavin reductase from *Thermus thermophilus* HB8, *J. Biol. Chem.* 286 (2011) 44078–44085, <https://doi.org/10.1074/jbc.M111.257824>.
- [60] H. Bisswanger, *Multisubstrate Reactions, Enzyme Kinetics: Principles and Methods*, Wiley-VCH, Weinheim, 2017.
- [61] K.B. Taylor, *Effects of Product Inhibitors, Enzyme Kinetics and Mechanisms*, Kluwer Academic Publishers, New York, 2004.
- [62] U. Kirchner, A.H. Westphal, R. Müller, W.J.H. van Berkel, Phenol hydroxylase from *Bacillus thermoglucosidius* A7, a two-protein component monooxygenase with a dual role for FAD, *J. Biol. Chem.* 278 (2003) 47545–47553, <https://doi.org/10.1074/jbc.M307397200>.
- [63] T.R. Russell, S.C. Tu, *Aminobacter aminovorans* NADH:flavin oxidoreductase His140: a highly conserved residue critical for NADH binding and utilization, *Biochemistry* 43 (2004) 12887–12893, <https://doi.org/10.1021/bi048499n>.